

USE OF DISSOLVED AND COLLOIDAL ACTINIDE PARAMETERS WITHIN THE 1996 WASTE
ISOLATION PILOT PLANT COMPLIANCE CERTIFICATION APPLICATION

Christine T. Stockman and Robert C. Moore

Sandia National Laboratories
PO Box 5800
Albuquerque, NM 87185-0733

Sandia is a multiprogram laboratory operated by Sandia Corporation, a Lockheed Martin Company, for the United States Department of Energy under contract DE-AC04-94AL85000.

1.0 Background

The Waste Isolation Pilot Plant (WIPP) is a geologic repository operated by the U.S. Department of Energy (DOE) for disposal of transuranic radioactive wastes. The repository is located near Carlsbad in southeast New Mexico, and is approximately 650 meters underground in the Salado Formation. The geologic formations immediately above and below the Salado are the Rustler and Castile Formations, respectively. The Rustler is considered important because it contains the most transmissive units above the repository; the most significant of these is considered to be the Culebra Dolomite members. The Castile contains areas of pressurized brine (brine pockets); it is not known whether any such pockets are located directly under the repository. The 16 square miles surrounding the shafts, surface facilities, and the underlying subsurface are controlled by the DOE.

In October 1996, the DOE submitted a compliance certification application (CCA) to the U.S. Environmental Protection Agency (EPA) in accordance with the requirements of Title 40 of the *Code of Federal Regulations* (40 CFR) Parts 191 and 194. The containment requirements in 40 CFR 191.13(a) specify that the disposal system is to be designed to provide a reasonable expectation that radionuclide releases to the accessible environment during 10,000 years are not likely to exceed specified limits (which are based on the radionuclide inventory in the repository). The demonstration of having a reasonable expectation is to be based on a performance assessment (PA), which is defined in 40 CFR 191.12 as,

...an analysis that: (1) Identifies the processes and events that might affect the disposal system; (2) examines the effects of these processes and events on the performance of the disposal system; and (3) estimates the cumulative releases of radionuclides, considering the associated uncertainties, caused by all significant processes and events. These estimates shall be incorporated into an overall probability distribution of cumulative release to the extent practicable.

The accessible environment is defined as:

(1) the atmosphere, (2) land surfaces, (3) surface waters, (4) oceans, and (5) all of the lithosphere that is beyond the controlled area.

DISCLAIMER

This report was prepared as an account of work sponsored by an agency of the United States Government. Neither the United States Government nor any agency thereof, nor any of their employees, make any warranty, express or implied, or assumes any legal liability or responsibility for the accuracy, completeness, or usefulness of any information, apparatus, product, or process disclosed, or represents that its use would not infringe privately owned rights. Reference herein to any specific commercial product, process, or service by trade name, trademark, manufacturer, or otherwise does not necessarily constitute or imply its endorsement, recommendation, or favoring by the United States Government or any agency thereof. The views and opinions of authors expressed herein do not necessarily state or reflect those of the United States Government or any agency thereof.

DISCLAIMER

Portions of this document may be illegible electronic image products. Images are produced from the best available original document.

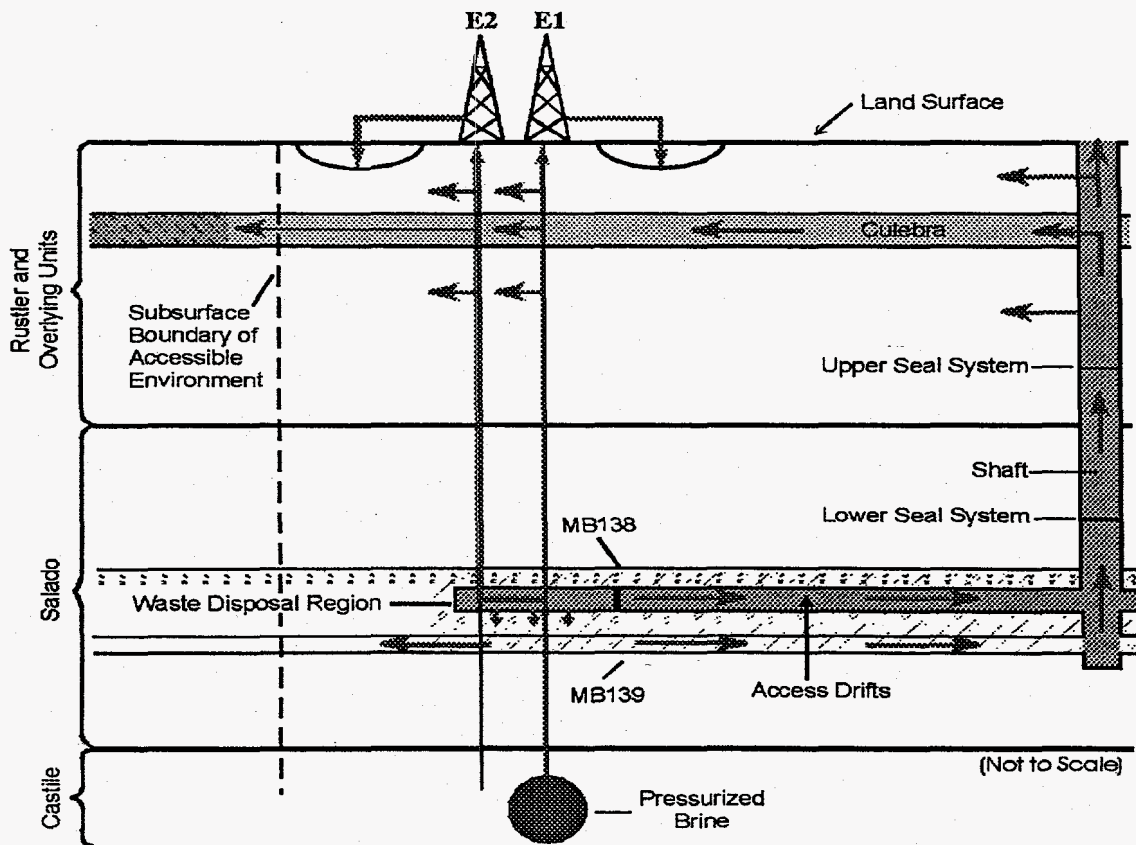
Many of the papers in this volume present detailed descriptions of the chemical analyses and methodologies that have been used to evaluate the maximum dissolved and colloid concentrations of actinides within the WIPP repository as part of the performance assessment. This paper describes the program for collecting experimental data and provides an overview of how the PA modeled the release of radionuclides to the accessible environment, and how solubility and colloid parameters were used by the PA models.

2.0 Release Mechanisms

Computer simulations predict that there will be essentially no release of radionuclides to the accessible environment in 10,000 years if the repository is left undisturbed. However, the controlling regulations, 40 CFR191 and 40CFR194, require the evaluation of inadvertent intrusions, such as exploratory drilling for oil, and it is these intrusions and their possible releases of contaminated brine that are of concern. Figure 1 shows a conceptual view of the repository and possible release paths.

While searching for natural resources (oil) in the deeper formations of the region, drillers may penetrate the repository. A pressurized brine pocket may or may not be present in these lower formations, leading to uncertainty as to whether a brine pocket is encountered. If the repository is breached, the drill bit will cut through the waste and the drilling fluids will carry the solid radioactive materials directly to the surface and into the drilling mud pit. In addition, if the repository is at least half filled with brine and under high pressure at the time of drilling, contaminated brine may be forced up the drill hole and into the mud pit. As specified in the EPA regulations, it is assumed that no natural resources will be found and that present-day standards for plugging and abandoning the drill holes will be used. After 200 years, the cement borehole plugs are assumed to degrade to a material with a permeability equivalent to silty sand, and contaminated brine may flow up the borehole and into the Culebra dolomite. From this point, the contaminated brine may travel beyond the controlled area and be used for livestock and/or agricultural purposes.

Thus there are three mechanisms for release of radionuclides to the accessible environment: direct release (DR) of solids during drilling, direct release of contaminated brine during drilling, and long-term release (LR) of contaminated brine through the Culebra dolomite. For the last two mechanisms, it is necessary to determine the concentration of radionuclides that may be mobilized into the brine phase. This was accomplished using solubility and colloid parameters experimentally determined by the actinide source term group.



Note: Example shown includes only two boreholes, both of which penetrate waste and one of which penetrates pressurized brine in the underlying Castile Formation. Pathways are similar for examples containing multiple boreholes. Arrows indicate hypothetical direction of groundwater flow and radionuclide transport.

- | | | |
|-------------------------------|---|--|
| Anhydrite layers a and b | Groundwater flow and radionuclide transport | Repository and shafts |
| Culebra | Disturbed rock zone | Increase in Culebra hydraulic conductivity due to mining |

CCA-012-2

Figure 6-12. Conceptual Release Pathways for the Disturbed Performance Deep Drilling Scenario E1E2

Figure 1. Conceptual view of WIPP repository and possible human intrusion. (DOE, 1996, Vol 1, Chapter 6, p 79))

3.0 Models and Codes Used in the Assessment

The performance assessment required the calculation of complementary cumulative distribution functions (CCDFs), which are ordered sets of points that span the cumulative normalized releases from the waste isolation system for all combinations of future histories of the repository over the 10,000-year regulatory period. The cumulative normalized releases are calculated by summing over time the releases of all regulated isotopes normalized by their release limits. The CCDF is compared with the quantitative release limits specified in 40 CFR § 919.13(a) to determine compliance.

Because of the large number of complex calculations required to produce CCDFs, components and subsystems of the WIPP were modeled in separate steps. Several computer

codes were used to simulate the relevant features of the disposal system and calculate the consequences for different scenarios.

Ten codes were used to model different aspects of brine flow and radionuclide transport for the three release mechanisms. Figure 2 is a flow diagram of the codes used in performance assessment. For long-term release, BRAGFLO was used to model flow of gas and brine within the Castile and Salado formations and up to the Culebra (Vaughn, 1996). NUTS and PANEL were used to model transport of radionuclides within the BRAGFLO brine flow. (Stockman et al., 1996) SECOFL was used to model fluid flow within the Culebra using transmissivity fields generated by GRASP_INV, and SECOTP was used to model transport within the SECOFL flow fields. (Ramsey et al., 1996) For brine direct release, the BRAGFLO flow fields were read by BRAGFLO (version 4.01), which calculated the volume of brine released during the exploratory drilling. (Stoelzel et al., 1996) PANEL was used again for the direct brine release to obtain the inventory of radionuclides per volume of brine as a function of time. CUTTINGS_S (Berglund, 1996) was used to calculate the volume of solid waste brought to the surface and EPAUNI (Sanchez et. al. 1997) was used to calculate the radionuclide inventory per waste volume. The output from all of these codes was brought together by the complementary cumulative distribution function grid flow code (CCDFGF) (Smith et al., 1996), to calculate releases to the accessible environment from the three mechanisms and produce the CCDF. Of these codes, only NUTS and PANEL used solubility and colloid concentration parameters to determine mobilized actinide concentrations within the brine. The other transport code, SECOTP, used the conservative assumption of no precipitation, and thus did not need these parameters.

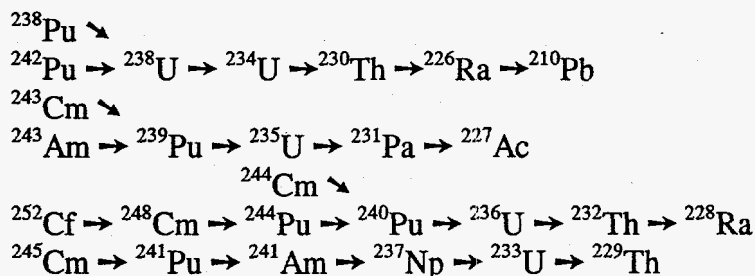
Both NUTS and PANEL assumed, at each time step, instant mobilization of radioisotopes up to their solubility limits if inventory was sufficient, or up to their inventory limits if inventory was insufficient (below effective solubility limits). The total inventory contained within the repository was assumed to be homogeneously and uniformly distributed throughout. NUTS assigned portions of the inventory to each grid block on the basis of that block's volume fraction of the repository as a whole. PANEL did the same, but it treated an entire waste panel as its one and only grid block. Thus both codes required input of the repository inventory of each modeled isotope and the solubility for each modeled element. Although both codes were originally designed to mobilize and transport dissolved species, they may also be used to mobilize and transport any species that may be characterized by a maximum concentration and inventory. Actinides within the WIPP are expected to be mobilized into the brine phase as dissolved species and four types of colloidal species: actinide intrinsic colloids, humic colloids, mineral fragment colloids, and microbe colloids. Thus a method for representing these five species within the calculations had to be chosen.

Colloids may transport differently than dissolved species because of a number of physical processes such as diffusion, filtration, and sorption. (Stumm, 1992; Morel and Herring, 1993; Vold and Vold, 1993) In calculations where these processes are important, such as the SECOTP calculations of transport within fractured dolomite, colloids may transport very differently from dissolved species. Consequently, transport of dissolved and colloidal actinides were calculated separately in SECOTP. For transport through the degraded waste panels and boreholes, however, these processes would change with time and be very difficult to quantify. Consequently, the project decided not to take any credit for diffusion, filtration, or sorption within the Salado formation. Because no physical mechanisms which could transport the species differently were modeled in the NUTS and PANEL calculations, all five species were "lumped" together. A single

“effective solubility” was assigned for each actinide; this was the sum of the solubility and the maximum steady-state colloid concentrations. After transport through the Salado formation, the actinides were “broken out” into their dissolved and colloidal components for transport through the Culebra formation.

4.0 Radioisotopes Included in the Performance Assessment

Of the 135 radioisotopes reported in the Waste Isolation Pilot Plant Transuranic Waste Baseline Inventory Report (DOE, 1995), 47 are regulated by 40 CFR 191. Sanchez et al. (1997) compiled a projected WIPP inventory of these isotopes and reported their results in curies and EPA units (an EPA unit is defined as the inventory of that isotope in curies divided by the EPA release limit for that isotope in curies as specified in 40 CFR Part 191, Appendix A, Table 1). The repository is considered to comply with the EPA regulations if there is less than a 0.1 probability that the cumulative release to the accessible environment is greater than 1 EPA unit, and less than a 0.001 probability that the cumulative release is greater than 10 EPA units.) Of the 135 isotopes listed, only 24 have more than 0.001 EPA units of inventory at any time within the 10,000-year regulatory period. Consequently, only those have a direct potential to affect calculated releases. In addition to those, however, there are several unregulated short-lived isotopes that (1) have significant inventory, and (2) decay to regulated isotopes. The radioisotopes that could affect regulated releases indirectly have long been included in the list of 30 radioisotopes treated by PANEL. The two lists, i.e., the 24-member list of top EPA-unit isotopes and PANEL’s list of 30 isotopes, were combined. Because of overlap, the amalgamated list included a total of 33 distinct isotopes, and these were considered for inclusion in the 1996 CCA PA. Table 1 lists these isotopes in order of maximum EPA units over the 10,000-year regulatory period. All of the 33 radionuclides except ^{14}C , ^{137}Cs , ^{147}Pm , ^{147}Sm , ^{90}Sr , and ^{232}U belong to the following decay chains¹:



¹ These decay chains were simplified by leaving out the many very short-lived and therefore unregulated intermediates. Leaving out short-lived intermediates that lie between regulated isotopes does not affect the rate of decay and ingrowth of the remaining long-lived isotopes. This is demonstrated by the verification of PANEL’s simplified decay chains against ORIGEN’s full decay chains in PANEL’s software quality assurance documents.

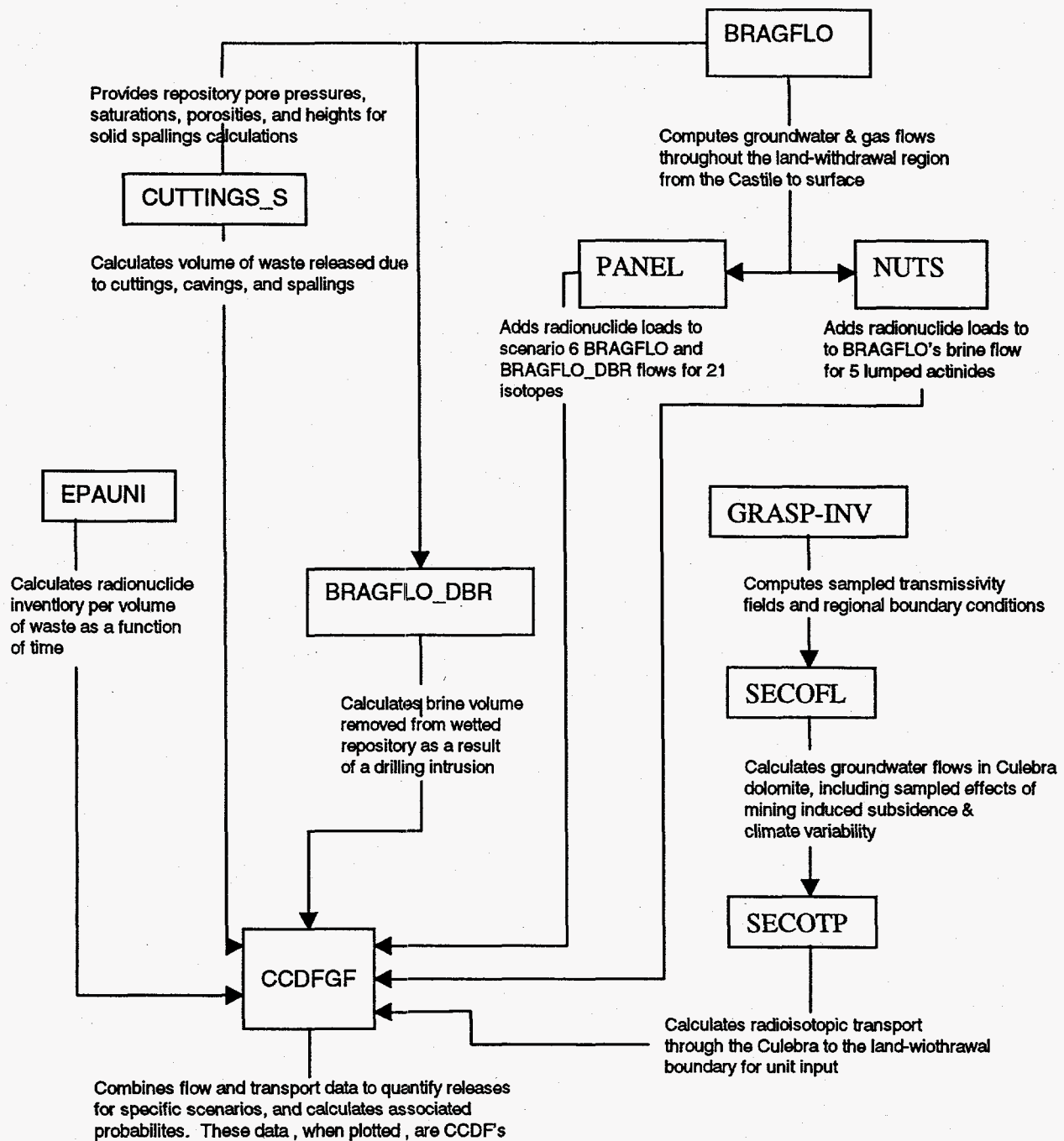


Figure 2. Flow Diagram of the Computer Codes used for Performance Assessment of the WIPP (Stockman et al., 1996)

Short-lived isotopes like ^{238}Pu decay quite rapidly, dropping to less than an EPA unit by 1100 years, while other isotopes like ^{230}Th that initially have low EPA units grow to over an EPA unit in 10,000 years. Some isotopes at the bottom of the table have short half-lives and are not regulated by the EPA, but they also have significant curies and are the parents of regulated isotopes, so they were included in the calculations.

The number of isotopes had to be reduced for the computationally intensive codes because each isotope that is included increases the calculation time. The first three columns in Table 1 show which isotopes were included in the calculations done by EPAUNI (solid direct

Table 1. The 33 Isotopes Considered for Modeling in the 1996 CCA PA [Based on the data reported in the Analysis Report for EPAUNI (Sanchez et al., 1997)]

SOLID	PANEL	NUTS			Half life	Release	0 years	0 years	100 years	350 years	10,000 yr.	
DR	DR+LR	LR		Isotope	(years)	Limit (Ci)	Ci	EPA Units ²	EPA Units	EPA Units	EPA Units	MAX EPA
x	x	x	t,p	Pu-238	8.77E+01	344	1.94E+06	5.64E+03	2.55E+03	3.55E+02	1.32E-22	5.64E+03
x	x	x	t,p	Pu-239	2.41E+04	344	7.95E+05	2.31E+03	2.31E+03	2.29E+03	1.73E+03	2.31E+03
x	x	x	t,p	Am-241	4.32E+02	344	4.88E+05	1.42E+03	1.24E+03	8.31E+02	1.78E-04	1.42E+03
x	x	c	t,p	Pu-240	6.54E+03	344	2.14E+05	6.22E+02	6.16E+02	6.02E+02	2.16E+02	6.22E+02
x			t,p	Cs-137	3.00E+01	3440	9.31E+04	2.71E+01	2.69E+00	8.31E-03	0.00E+00	2.71E+01
x			t,p	Sr-90	2.91E+01	3440	8.73E+04	2.54E+01	2.35E+00	6.10E-03	0.00E+00	2.54E+01
x	x	c	t,p	U-233	1.59E+05	344	1.95E+03	5.67E+00	5.67E+00	5.67E+00	5.44E+00	5.67E+00
x	x	x	t,p	U-234	2.45E+05	344	7.51E+02	2.18E+00	3.28E+00	4.07E+00	4.10E+00	4.10E+00
	x	x	t,p	Th-230	7.70E+04	34	3.06E-01	8.90E-03	3.40E-02	1.19E-01	3.55E+00	3.55E+00
	x	c	t,p	Pu-242	3.76E+05	344	1.17E+03	3.40E+00	3.40E+00	3.40E+00	3.34E+00	3.40E+00
	x	c	t,p	Th-229	7.34E+03	344	9.97E+00	2.90E-02	8.20E-02	2.12E-01	3.40E+00	3.40E+00
	x		t,p	Np-237	2.14E+06	344	6.49E+01	1.89E-01	2.32E-01	3.14E-01	4.83E-01	4.83E-01
			t,p	Ra-226	1.60E+03	344	1.14E+01	3.31E-02	3.20E-02	2.94E-02	2.77E-01	2.77E-01
			t,p	Pb-210	2.23E+01	344	8.75E+00	2.54E-02	3.20E-02	2.97E-02	2.77E-01	2.77E-01
	x		t,p	U-238	4.47E+09	344	5.01E+01	1.46E-01	1.46E-01	1.46E-01	1.46E-01	1.46E-01
	x		t,p	U-236	2.34E+07	344	6.72E-01	1.95E-03	3.78E-03	8.28E-03	1.16E-01	1.16E-01
	x		t,p	Am-243	7.37E+03	344	3.25E+01	9.45E-02	9.36E-02	9.16E-02	3.69E-02	9.45E-02
	x		t,p	U-235	7.04E+08	344	1.75E+01	5.09E-02	5.12E-02	5.15E-02	7.06E-02	7.06E-02
	x		t,p	Cm-243	2.91E+01	344	2.07E+01	6.02E-02	5.29E-03	1.21E-05	0.00E+00	6.03E-02
			t	U-232	6.89E+01	344	1.79E+01	5.20E-02	1.99E-02	1.79E-03	0.00E+00	5.20E-02
			t	C-14	5.72E+03	344	1.28E+01	3.72E-02	3.69E-02	3.58E-02	1.11E-02	3.72E-02
	x		t,p	Th-232	1.41E+10	34	1.01E+00	2.94E-02	2.94E-02	2.94E-02	2.94E-02	2.94E-02
			t	Ac-227	2.18E+01	344	5.05E-01	1.47E-03	1.44E-03	1.69E-03	1.28E-02	1.28E-02
			t,p	Pa-231	3.28E+04	344	4.67E-01	1.36E-03	1.46E-03	1.72E-03	1.28E-02	1.28E-02
	x		p	Cm-248	3.39E+05	344	3.72E-02	1.08E-04	1.08E-04	1.08E-04	1.06E-04	1.08E-04
	x		p	Cm-245	8.53E+03	344	1.17E-02	3.40E-05	3.52E-05	3.66E-05	1.85E-05	3.66E-05

² An EPA unit is a normalized unit obtained by dividing the curies of an isotope by the EPA release limit (in curies) for that isotope.

	x		p	Pu-244	8.26E+07	344	1.51E-06	4.39E-09	4.48E-09	4.68E-09	1.26E-08	1.26E-08
			p	Sm-147	1.06E+11	344	4.55E-10	1.32E-12	1.32E-12	1.32E-12	1.32E-12	1.32E-12
			p	Pm-147	2.62E+00		8.10E-04					
			p	Ra-228	5.75E+00		1.00E+00					
			p	Cf-252	2.64E+00		1.72E-04					
x	x		p	Cm-244	1.81E+01		7.44E+03					
x	x	c	p	Pu-241	1.44E+01		3.94E+05					
0.9996	0.9948	0.9947	:fraction of total EPA units at closure									

x = included in calculation,
c = combined with a transported isotope
t = one of top 24 isotopes
p = one of PANEL isotopes

release), PANEL (long-term and direct release), and NUTS (long-term release). For the EPAUNI calculations of direct solid release, waste was categorized into more than 500 waste streams based on the source and inventory of the waste. After all of the waste inventories were examined, the top 8 isotopes in Table 1 were chosen (indicated with an x in the table), along with two short-lived parents of these 8 isotopes because these isotopes dominate the inventory in all waste streams and account for 99.96% of the EPA units at the time of closure of the repository in 2033 A.D. For the faster-running code PANEL, it was possible to use more isotopes. Twenty-one isotopes were used for the PANEL brine release calculations, totaling 99.48% of the EPA units at closure. In the NUTS calculations, only five isotopes were directly modeled, as indicated by the x in the third column, but five additional isotopes were indirectly modeled by "lumping" their inventory with modeled isotopes with similar decay and transport properties. The resulting 10 isotopes account for 99.47% of the EPA units at closure. For the SECOTP, ²³⁸Pu was dropped from the list of five lumped isotopes because the amount of it calculated to be delivered to the Culebra was small.

5.0 Brine Composition

Actinide solubility and maximum actinide concentrations on colloids may vary significantly with oxidation state, pH, carbonate concentration, and brine composition. The pH and carbonate concentration within the repository were expected to be well controlled by the MgO backfill (Wang, 1996), leaving brine composition and oxidation state as the only major variables influencing solubility. Oxidation state is described in Section 6.3. Brine composition is described here.

The choice of brine compositions for modeling actinide solubility was determined by the brines present within the WIPP formations and the changes that would take place in their compositions when they enter the repository. There are three distinct brine compositions (Table 2) in the three WIPP formations (Salado, Castile, and Culebra sub-unit of the Rustler).

Under all scenarios, brine will flow from the surrounding Salado Formation through the disturbed rock zone (DRZ), and into the repository in response to the pressure difference between the repository at closure and the surrounding formation. In scenarios where a borehole is drilled into the repository but not into an underlying brine pocket, brine may flow down the borehole

from the Rustler and Dewey Lake Formations. In scenarios where a pressurized Castile brine pocket is penetrated, brine from the Castile Formation may flow up the borehole into the repository. In this case there is expected to be very little Culebra brine flow down the borehole before the repository is filled by Castile brine flowing up from the brine pocket.

The composition of the more dilute brines of the Rustler and Dewey Lake Formations is expected to change rapidly when it enters the repository due to fast dissolution of host Salado Formation minerals (about 93.2% halite and about 1.7% each of polyhalite, gypsum, anhydrite, and magnesite; Brush, 1990). If the dilute brines dissolve only the surfaces of the repository, they will attain Castile-like compositions, but if they circulate through the Salado Formation after saturating with halite, they may attain compositions within the range for Salado brine. The actual brine within the repository may be described as a mixture of the two concentrated brine "end members" -- Salado and Castile. The brine ratio in this mixture is, however, difficult to quantify,

Table 2. Major Chemical Components of WIPP Brines (Brush, 1990)

Element or Chemical Property	Salado (Brine A)	Castile (ERDA-6)	Culebra (Air Intake Shaft)
HCO ₃ ⁻ (mM)	--	43	1.1
B ³⁺ (mM)	20	63	2.8
Br ⁻ (mM)	10	11	0.37
Ca ²⁺ (mM)	20	12	23
Cl ⁻ (mM)	5350	4800	567
K ⁺ (mM)	770	97	8.3
Mg ²⁺ (mM)	1440	19	23
Na ⁺ (mM)	1830	4870	600
SO ₄ ²⁻ (mM)	40	170	77
pH	6.5	6.17	7.7
Total Dissolved Solids (mg/liter)	306,000	330,000	42,600

since it is both temporally and spatially variable. Only in the undisturbed scenario is the mixture well defined as 100% Salado brine over the 10,000-year time period. In the borehole intrusion scenarios, it is expected that the fraction of Salado brine within the mixture will be high in areas of the repository distant from the borehole and much lower near the borehole.

As seen in Table 2, Salado and Castile brines have different compositions, most notably in the Mg²⁺ concentration and ionic strength. These differences can cause significant differences in the actinide solubilities. Even after equilibrating with the MgO backfill, Salado brine has higher Mg²⁺ concentration and ionic strength than Castile. The higher ionic strength stabilizes highly charged actinide species, resulting in higher solubilities in some cases.

Since radioisotope transport up the borehole is required for significant release, it is the solubility of radioisotopes near the borehole that is most important. Given these uncertainties, and NUTS's requirement for time-independent solubilities, calculation of brine mixing was not attempted in the CCA calculations. Instead, actinide solubilities calculated in Castile brine were used for scenarios where a borehole hit a pressurized brine pocket and solubilities calculated in

Salado brine were used for scenarios where it did not. This simplification should bracket the range of behavior of the repository and should therefore suffice for CCDF calculations.

6.0 Parameters Used to Calculate the "Effective Solubilities" of the Actinides

The parameters required for constructing the "effective solubility" were: (1) modeled solubilities for four oxidation states in each end-member brine, (2) a distribution of the uncertainty in the model solubility values, (3) the scheme for assigning sampled dominant oxidation states, (4) colloidal concentrations or proportionality constants for the 6 actinides and the 4 oxidation states for each of four colloid types, and (5) upper limits on the actinide concentrations that may be carried on two colloid types.

6.1 Solubility Modeling

There are numerous models for accurately calculating equilibrium concentrations in low ionic strength aqueous solutions; however, few can adequately describe solution behavior in concentrated electrolytes. The activity coefficient formalism of Pitzer (1991) has been parameterized for concentrated aqueous electrolyte systems by Harvie-Møller-Weare (HMW, Harvie et al., 1984), who have demonstrated the reliability of this formalism for predicting mineral solubility using chemical equilibrium in electrolyte solutions from zero to high ionic strength. The database developed by Harvie et al. (1984) includes all parameters necessary to predict equilibrium in the Na^+ - K^+ - H^+ - Ca^{2+} - Mg^{2+} - OH^- - SO_4^{2-} - HSO_4^- - Cl^- - HCO_3^- - CO_3^{2-} - CO_2 - H_2O system. This database serves as the reference database for the parameterization of the WIPP model.

The Pitzer ion-interaction model (Pitzer, 1973, 1991) is a semiempirical model for calculating activity coefficients for high ionic strength, and has been proven accurate for calculating solubilities in multicomponent electrolyte solutions (Harvie et al., 1984). In the Pitzer model, the excess free energy is represented by combining a modified Debye-Hückel equation for the dilute solution region with a virial expansion for higher ionic concentrations. The model can be reliably extended to multicomponent systems using parameters derived from binary and ternary systems (Harvie and Weare, 1980; Harvie et al., 1984).

The Pitzer model has been successfully used with marine evaporite systems (Harvie et al., 1980; Eugster et al., 1980; Brantley et al., 1984) mineral precipitation in lakes (Spencer et al., 1985; Felmy and Weare, 1986), and actinide solubility in high ionic strength brines (Novak et al., 1996; Al Mahamid et al., 1998). Pitzer (1991) gives a complete description of the formalism and model parameters for many ionic species.

6.1.1 Parameterization of the Pitzer model and Solubility Calculations.

Pitzer parameters or data used to calculate Pitzer parameters for actinides in the +III oxidation state in high ionic strength brines have been reported by Fanghänel et al., 1994; Felmy et al., 1995; Felmy et al., 1990; Felmy et al., 1989; Novak et al., 1995; Rai et al., 1992a,b; Rai et al., 1995a; and Rao et al., 1996. Data or Pitzer parameters for actinides in the +IV oxidation state have been reported by Felmy and Rai, 1992; Felmy et al., 1991; Felmy et al., 1997; Rai et al.,

1995b; and Rai et al., 1997. Data or Pitzer parameters for actinides in the +V oxidation state have been reported by Novak and Roberts, 1995; Al Mahamid et al., 1998; Roy et al., 1992; Fanghänel et al., 1995; and Neck et al., 1995. Stability constants for actinide-organic ligands have been reported by Pokrovsky et al., 1998; Novak et al., 1996; and Martell and Smith, 1977. Data for much of the organic ligand work performed for WIPP has either already been published in the literature (including this volume) or will be published in the near future. The ligands investigated in this work included acetate, lactate, oxalate, citrate, and ethylenediamine tetraacetic acid (EDTA). These compounds were chosen for their aqueous solubility and because they were expected to be present in WIPP waste. Empirical solubility experiments to test and challenge the WIPP solubility model are under way at Argonne National Laboratory and at Pacific Northwest National Laboratory (PNNL). The papers in this volume describe some of the experimental methods and procedures used to determine the data.

Experiments were conducted with one actinide for each of the four possible oxidation states and, through the oxidation state analogy (in which actinides in the same oxidation state tend to exhibit similar behavior), bounding models were developed to represent each oxidation state of the actinides. The actinides for which data were obtained americium, thorium, neptunium, and uranium in the +III, +IV, +V, and +VI oxidation states, respectively. For example, the solubility of Pu in the +III and +IV states was represented by the solubility of Am(III) and Th(IV). Sufficient data have been collected to parameterize the model for +III, +IV, and +V actinides. Data for +VI are still being developed. Since a complete model for +VI actinides was unavailable, literature data from empirical solubility studies for U(+VI) were used to determine a +VI actinide solubility. The use of solubility bounding analogs for each oxidation state instead of actual values for each element in each oxidation state required fewer experiments and greatly simplified the solubility model. Because the analogs provide a bounding case for each oxidation state, the model always predicts conservative values for actinide solubilities that were used in WIPP performance assessment calculations.

The experimental data were used to calculate Pitzer parameters and standard chemical potentials using the NONLIN V2.0m software, which is a Gibbs energy minimization routine developed by A. Felmy at PNNL. The complete parameterized database was used in conjunction with the FMT V2.0 aqueous speciation computer code developed by C. Novak at Sandia National Laboratories for use on a DEC/Alpha platform to predict maximum actinide equilibrium solubilities in Salado and Castile brines. Organic ligands were not included in solubility calculations. Utilizing the results of organic ligand experiments at Florida State University, divalent cations (e.g., Mg^{2+} , Ca^{2+} , Fe^{2+} , Ni^{2+}) ions present in large quantities in the disposal room have been shown to compete with the actinides for complexation with the ligands. The effect is that actinide concentrations will not be significantly enhanced by the presence of organic ligands (Department of Energy, 1996). Calculations for both Salado and Castile brines were performed assuming the brines were equilibrated with MgO backfill. Sufficient MgO backfill will be emplaced with the waste to react quickly with any microbially produced CO_2 , preventing a drop in pH and a rise in dissolved carbonate species. The results for actinide solubility calculations for each oxidation state are given in Table 3.

Table 3. Modeled Solubilities for Actinides in the Four Oxidation States and Two Brines [pH and $f(\text{CO}_2)$ controlled by the $\text{Mg}(\text{OH})_2$ - MgCO_3 buffer] (DOE, 1996, appendix SOTERM)

	+IV	+V	+VI
Salado	4.4e-06	2.3e-06	8.7e-06
Castile	6.0e-09	2.2e-06	8.8e-06

6.2 Distributions

After the model solubilities were obtained from Novak and Moore (1996), solubility distributions were calculated by Bynum (1996), who compared calculated solubilities with those observed experimentally and prepared a distribution of the divergence of model solubilities from experimental results. Figure 3 shows the distributions of the observed solubilities around the model solubilities and is plotted as the log of the molar concentration. It can be seen that the observed solubilities are up to 2 orders of magnitude lower than those calculated by the model and in some cases are up to 1.4 orders of magnitude above the model solubilities. These values were used as the total uncertainty in mode predicted solubility. Uncertainties in the model and the data were not treated as separate, but were "lumped" into parameter uncertainty. The information was entered into the parameter database as the actual points on the cumulative distribution.

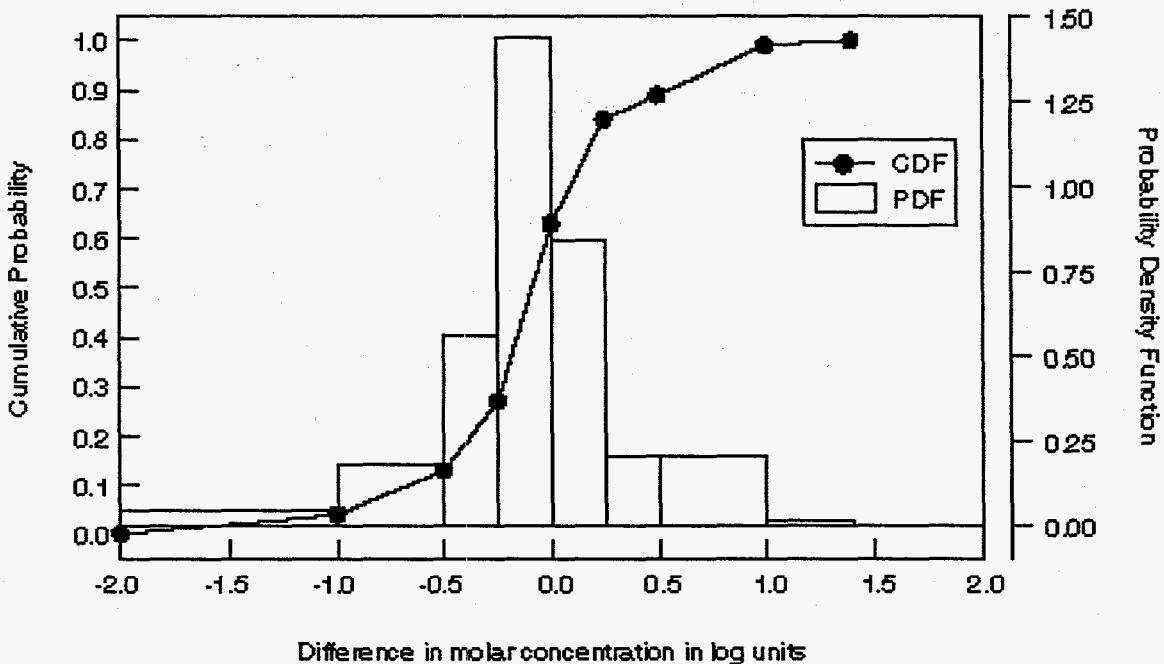


Figure 3. Distribution of actinide log solubilities. (Bynum, 1996)

6.3 Oxidation States

The solubilities of actinides are dependent on the actinide oxidation-state distributions (Weiner, 1996), which are expected to be determined by reactions of the actinides with the major components of the waste. Microbially mediated reactions with the organic waste and anoxic corrosion of the steel waste containers, which results in the production of dissolved Fe(+II), are expected to have the largest impact on the oxidation-state distribution, but because the propensity of plutonium to exist in multiple oxidation states, and lack of redox data in concentrated brines, it is impossible to define a single redox state for the repository. It is expected that the redox state of the repository may range from "reducing" to "extremely reducing," and experiments (Weiner, 1996) have shown that for most of the actinides, high oxidation states will not persist. The most likely persistent oxidation states for the six actinides are shown in Table 4. For U, Np, and Pu, two oxidation states are possible under the anticipated repository conditions. While both may coexist, one will dominate the solubility. A bounding case was created through independent sampling of each oxidation state at its thermodynamic maximum solubility.

Table 4. Possible Oxidation States of Actinides Under Repository Conditions (DOE, 1996)

<u>Actinide</u>	<u>Oxidation State</u>
Am	+III
Cm	+III
Np	+IV, +V
Pu	+III, +IV
Th	+IV
U	+IV, +V

6.4 Colloid Parameters

Colloid parameters were obtained from Papenguth (1996a-d). These were of two types: the steady-state colloid actinide concentrations for mineral fragments and actinide intrinsic colloids, and proportionality constants for humic and microbe colloids. Proportionality constants indicated the amount of actinides on the humic or microbe colloids versus the concentrations in solutions. There were also concentration caps for those colloid types.

For the steady-state colloid actinide concentrations, Papenguth (1996a) provided a range of 2.6^{-10} to 2.6^{-8} moles per liter for Am, Pu, U, Th, and Np sorbed on mineral fragments. For actinide intrinsic colloids, Papenguth (1996b) provided a concentration of 10^{-9} M for Pu. The other actinide intrinsic colloids were not stable but agglomerated and settled out, so 0 M was used.

For humic and microbe colloids, Papenguth (1996c,d) provided proportionality constants and concentration upper limits or caps as shown below in Table 5. For humic colloids, the cap was based on the maximum steady-state number of sorption sites on the suspended humic colloids. For microbe colloids, the cap was based on the actinide concentration that was toxic to the microbes. Note that for microbe colloids, the proportionality constant is provided by the actinide element, but the humic proportionality constant is provided by the oxidation state and brine composition. A comparison of the WIPP data to literature data was not possible due to a lack of data for colloid actinide interactions under WIPP conditions in the literature.

Table 5. Proportional Constants and Concentration Upper Limits or Cap for Microbial and Humic Colloids Used in PA (DOE, 1996)

Microbial Colloids			
Actinide	Proportionality Constant		Cap
Am	3.6		^c
Pu	0.3		6.8e-5
U	2.1e-3		2.1e-3
Th	3.1		1.9e-3
Np	12		2.7e-3
Humic Colloids			
Total Actinide by Oxidation State	Proportionality Constant ^d		Cap ^b
	Salado	Castile	Both Brines
+III	0.008 to 0.19	0.065	1.1e-5
+IV	6.3	6.3	1.1e-5
+V	5.3e-5 to 9.1e-4	4.3e-4 to 7.4e-3	1.1e-5
+VI	0.008 to .12	0.062 to 0.51	1.1e-5

^a Moles of mobile microbial actinide (An) / moles dissolved An.

^b Cap on total moles mobile An / liter

^c High cap entered so that only inventory limit would cap Am mobilized on microbes (²⁴¹Am inventory limit = 538 moles / 3e+4m³ = 1.8e-5 M)

^d Moles of mobile humic-bound An / moles dissolved An.

6.5 Combining the Source Term Parameters into an Effective Solubility

Before use by NUTS and PANEL, the uncertain dissolved and colloidal parameters were sampled, resulting in 100 sample sets of parameters. For each sample set, the parameters were then combined into "effective solubilities" for each of the actinides as described below. Parameters that were sampled, and values derived from them, have been indicated by italics. Parameters read from the parameter database are in boldface type.

$$\text{Dissolved Solubility} = \text{Model Solubility} * 10^{\text{Sampled from Solubility Distribution}}$$

$$\text{Humic Colloid Concentration} = \text{Dissolved Solubility} * \text{Proportionality Constant}$$

if $\text{Dissolved} * \text{Prop. Const.} < \text{Humic Cap}$, otherwise
Humic Colloid Concentration = Humic Cap

$$\text{Microbe Colloid Concentration} = \text{Dissolved Solubility} * \text{Proportionality Constant}$$

if the $\text{Total Mobile} < \text{Microbe Cap}$, otherwise
Microbe Colloid Concentration = Microbe Cap

$$\text{Mineral Colloid Concentration} = \text{Database Concentration}$$

$$\text{Intrinsic Colloid Concentration} = \text{Database Concentration}$$

$$\text{Total Mobile} = \text{Dissolved} + \text{Humic} + \text{Microbe} + \text{Mineral} + \text{Intrinsic}$$

$$\text{LOGSOLM} = \log_{10}(\text{Total Mobile})$$

where LOGSOLM is the log of the "effective solubility" in moles/liter used by NUTS and PANEL. Table 7 shows LOGSOLM for each brine and oxidation state calculated using median values for all sampled parameters.

Table 6. Median "Effective Log Solubilities" for Each Brine and Oxidation State (DOE, 1996)

Brine	Am(+III), Cm(+III)	Pu(+III)	Pu(+IV)	U(+IV)	U(+VI)	Th(IV)	Np(IV)	Np(V)
Salado	-5.64	-6.14	-4.80	-4.84	-5.10	-4.59	-4.17	-4.52
Castile	-6.47	-6.77	-7.19	-7.16	-4.96	-7.05	-6.85	-4.54

For actinides with more than one oxidation state, the above procedure was performed for each oxidation state, and the final total mobile concentration is set based on the oxidation state parameter:

$$\begin{aligned} \text{Total mobile} &= \text{Total mobile(lower oxidation state)} \text{ if } \text{OXSTAT} \leq 0.5 \\ &= \text{Total mobile(higher oxidation state)} \text{ if } \text{OXSTAT} > 0.5 \end{aligned}$$

where OXSTAT is the oxidation-state parameter that is sampled uniformly from 0 to 1.

7.0 Results

The results of the sampling and the construction of the total dissolved and colloid concentrations resulting from one set of calculations in the compliance certification application are shown in Figure 4. One hundred realizations were binned into half order of magnitude solubilities. The figure shows the number of vectors in each half order of magnitude bin. The “effective solubilities” are shown for only Am and Pu, since they account for over 99% of the EPA units of the inventory throughout the 10,000-year regulatory period.

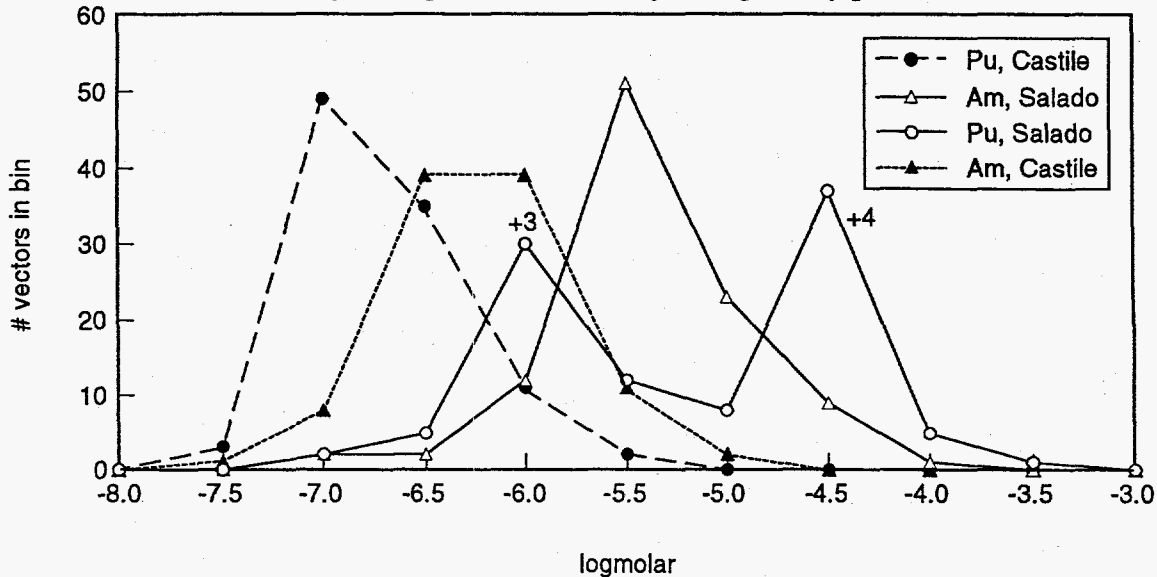


Figure 4. Total maximum log concentration (dissolved + colloid) Replicate 1. (DOE, 1996)

Figures 5 and 6 show the radionuclide concentrations in EPA units per cubic meter of brine as a function of time as calculated by PANEL for the direct brine release calculations. These concentrations are the sum of the concentrations of all 21 isotopes included in the PANEL calculation. In each of these figures, one can see four “regions.” (1) In the first several hundred years, there is a drop in the EPA unit concentrations of some realizations as the EPA units of ^{238}Pu decays to below that of ^{241}Am . (2) There is then a constant concentration seen for the period where ^{241}Am controls the total EPA unit concentration and is solubility limited. For the realizations that sampled a higher Am solubility, this period is shorter than for the realizations that sampled a lower Am solubility. (3) After the Am changes from solubility to inventory limited, the EPA unit concentration drops until (4) the ^{239}Pu solubility controls the EPA unit concentration. In region 4, the higher concentrations are constant but the lower concentrations show a slow decrease with time, because the sampled ^{239}Pu solubility is low enough that other isotopes which are inventory limited and have intermediate half-lives contribute to the total EPA unit concentrations. The spread in concentrations seen in region 2 reflects the spread in Am solubility, and the higher Am solubility in Salado brine than in Castile brine is clearly seen. Similarly, the region 4 spread mainly reflects the spread in Pu(+III) and Pu(+IV) solubilities. As can be seen,

the solubility of both oxidation states of Pu is quite low in Castile brine, but in Salado brine there is a bimodal distribution showing the higher solubility of Pu(+IV) and lower solubility of Pu(+III).

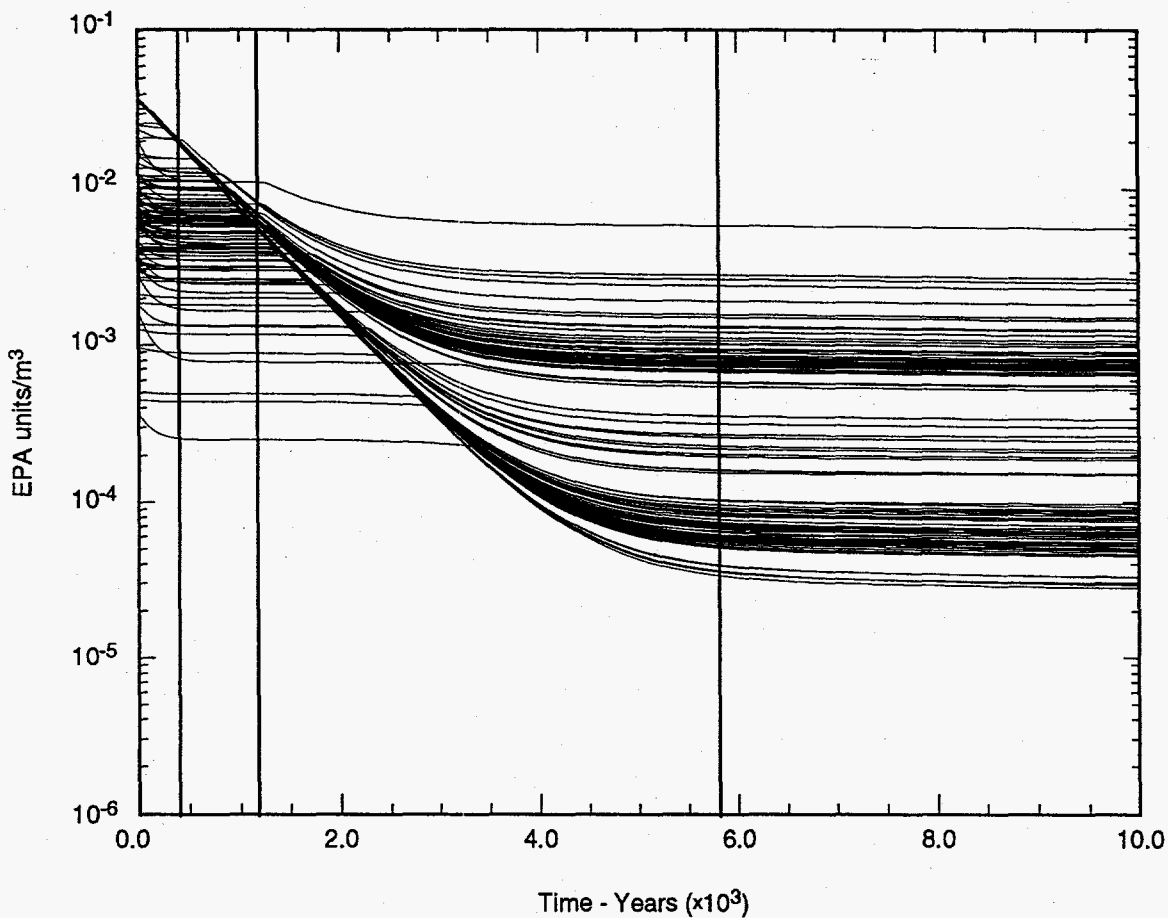


Figure 5. Radionuclide concentration in EPS units per m³ of Salado brine, as calculated by PANEL. (Stockman et al., 1996)

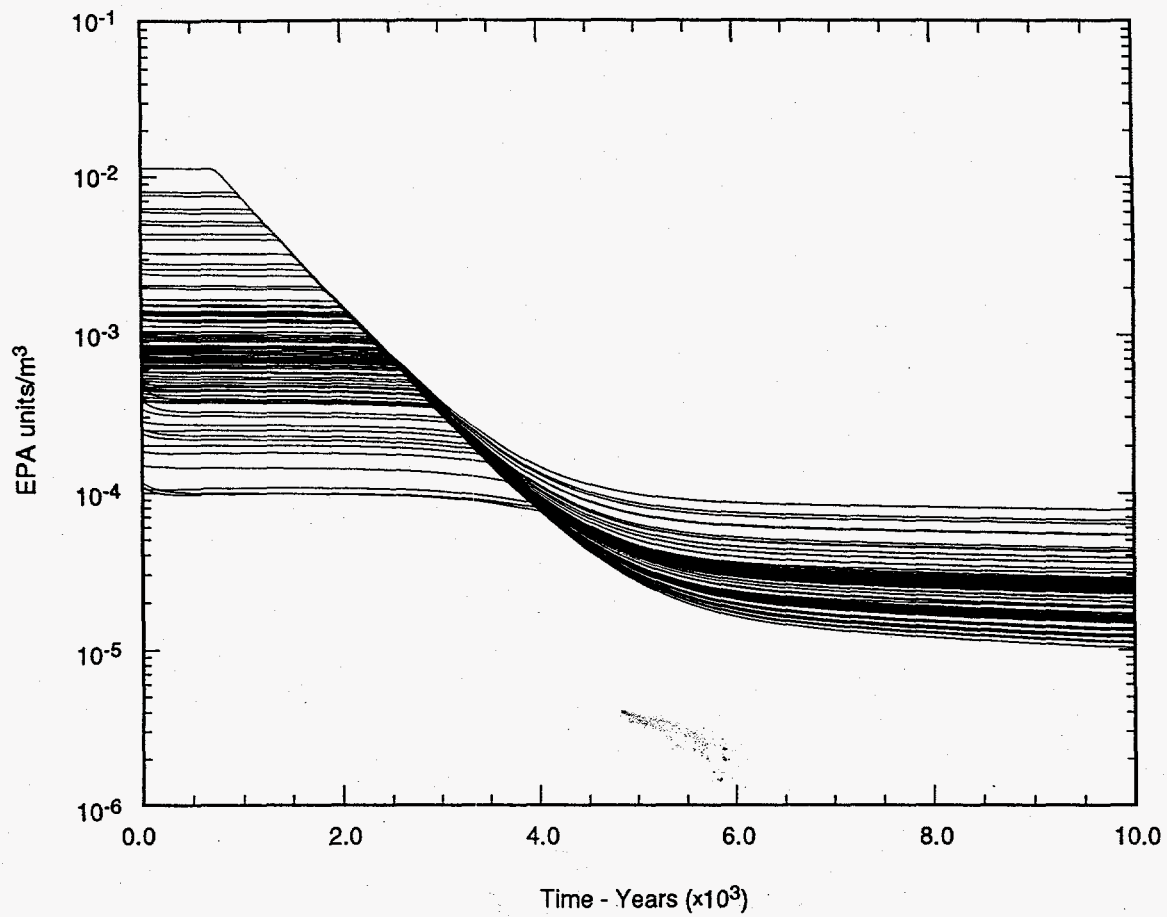


Figure 6. Radionuclide concentration in EPS units per m³ of Castile brine, as calculated by PANEL. (Stockman et al., 1996)

This work was supported by the United States Department of Energy under Contract DE-ACO4-94AL85000.

8.0 References

Note: Some of the work cited here (analysis packages) was prepared specifically for the Waste Isolation Pilot Plant and is available in the Sandia National Laboratories record center or the EPA public docket. Solubility and colloid work by Bynum, Papenguth, Weiner, and Wang also appear elsewhere in this volume.

Al Mahamid I., C.F. Novak, K.A. Becraft, S.A. Carpenter and N. Hakem. 1998. "Solubility of Np(V) in K-Cl-CO₃ and Na-K-Cl-CO₃ Solutions to High Concentrations: Measurements and Thermodynamic Model Predictions," *Radiochimica Acta* **81** 93-101.

Berglund, J.W. 1996. *Analysis Package for the Cuttings and Spallings Calculations (Task 5 and 6) of the Performance Assessment Calculation Supporting the Compliance Certification Application (CCA), AP-015 and AP-016*. Analysis Packages 15 and 16. Sandia National Laboratories, Albuquerque, NM. Sandia WIPP Central Files WPO# 40521.

Brantley, S.L., D.A. Crerar, N.E. Møller, and J.H. Weare. 1984. "Geochemistry of a Modern Marine Evaporite: Bocana de Virrila, Peru," *Journal of Sedimentary Petrology* **54** (2) 447-462.

Brush, L.H. 1990. *Test Plan for Laboratory and Modeling Studies of Repository and Radionuclide Chemistry for the Waste Isolation Pilot Plant*. SAND90-0266. Sandia National Laboratories, Albuquerque, NM.

Bynum, R.V. 1996. "Estimation of the Uncertainty for Predicted Actinide Solubilities." Sandia National Laboratories, Albuquerque, NM. Sandia WIPP Central Files WPO# 40512.

DOE (U.S. Department of Energy). 1995. *Waste Isolation Pilot Plant Transuranic Waste Baseline Inventory Report (Revision 2)*. DOE/CAO-95-1121, Revision 2. U.S. Department of Energy, Carlsbad Area Office, Carlsbad, NM.

DOE (U.S. Department of Energy). 1996. *Title 40 CFR Part 191 Compliance Certification Application for the Waste Isolation Pilot Plant*. DOE/CAO-96-2184, United States Department of Energy, Waste Isolation Pilot Plant, Carlsbad Area Office, Carlsbad, NM.

Eugster, H.P., C.E. Harvie, and J.H. Weare. 1980. "Mineral Equilibria in the Six-Component Seawater System, Na-K-Mg-Ca-Cl-SO₄-Cl-H₂O, at 25°C," *Geochimica et Cosmochimica Acta* **44** (9) 1335-1348.

Fanghänel, Th., J.I. Kim, P. Paviot, R. Klenze, and W. Hauser. 1994. "Thermodynamics of Radioactive Trace Elements in Concentrated Electrolyte Solutions: Hydrolysis of Cm³⁺ in NaCl-Solutions," *Radiochimica Acta* **66/67** 91-97.

Fanghänel, Th., V. Neck, and J.I. Kim. 1995. "Thermodynamics of Neptunium(V) in

Concentrated Salt Solutions. I. Ion Interaction (Pitzer) Parameters for Np(V) Hydrolysis Species and Carbonate Complexes," *Radiochimica Acta* **69** (3) 169-176.

Felmy, A.R., and D. Rai. 1992. "An Aqueous Thermodynamic Model for a High Valence 4:2 Electrolyte $\text{Th}^{4+}\text{-SO}_4^{2-}$ In the System $\text{Na}^+\text{-K}^+\text{-Li}^+\text{-NH}_4^+\text{-Th}^{4+}\text{-SO}_4^{2-}\text{-HSO}_4^-\text{-H}_2\text{O}$ to High Concentration," *Journal of Solution Chemistry* **21** (5) 407-423.

Felmy, A.R., and J.H. Weare. 1986. "The Prediction of Borate Mineral Equilibria in Natural Waters: Application to Searles Lake, California," *Geochimica et Cosmochimica Acta* **50** (12) 2771-2783.

Felmy, A.R., D. Rai, J.A. Schramke, and J.L. Ryan. 1989. "The Solubility of Plutonium Hydroxide in Dilute Solution and in High-Ionic-Strength Chloride Brines," *Radiochimica Acta* **48** (1/2) 29-35.

Felmy, A.R., D. Rai, and R.W. Fulton. 1990. "The Solubility of $\text{AmOHCO}_3(\text{c})$ and the Aqueous Thermodynamics of the System $\text{Na}^+\text{-Am}^{3+}\text{-HCO}_3^-\text{-CO}_3^{2-}\text{-OH}^-\text{-H}_2\text{O}$," *Radiochimica Acta* **50** (4) 193-204.

Felmy, A.R., D. Rai, and M.J. Mason. 1991. "The Solubility of Hydrated Thorium(IV) Oxide in Chloride Media: Development of an Aqueous Ion-Interaction Model," *Radiochimica Acta* **55** (4) 177-185.

Felmy, A.R., D. Rai, M.J. Mason, and R.W. Fulton. 1995. "The Aqueous Complexation of Nd(III) with Molybdate: The Effects of Both Monomeric Molybdate and Polymolybdate Species," *Radiochimica Acta* **69** (3) 177-183.

Felmy, A.R., D. Rai, S.M. Sterner, M.J. Mason, N.J. Hess, and S.D. Conradson. 1997. "Thermodynamic Models of Highly Charged Aqueous Species: Solubility of Th(IV) Hydrated Oxide in Concentrated NaHCO_3 and Na_2CO_3 Solutions." *Journal of Solution Chemistry* **26** (3) 233-248.

Harvie, C.E., and J.H. Weare. 1980. "The Prediction of Mineral Solubilities in Natural Waters: the $\text{Na-K-Mg-Ca-Cl-SO}_4\text{-H}_2\text{O}$ System from Zero to High Concentration at 25°C," *Geochimica et Cosmochimica Acta* **44** (7) 981-997.

Harvie, C.E., J.H. Weare, L.A. Harvie, and H.P. Eugster. 1980. "Evaporation of Seawater: Calculated Mineral Sequences," *Science* **208** (4443) 498-500.

Harvie, C.E., N.E. Møller, and J.H. Weare. 1984. "The Prediction of Mineral Solubilities in Natural Waters: The $\text{Na-K-Mg-Ca-H-Cl-SO}_4\text{-OH-HCO}_3\text{-CO}_3\text{-CO}_2\text{-H}_2\text{O}$ System to High Ionic Strengths at 25°C," *Geochimica et Cosmochimica Acta* **48** (4) 723-751.

Harvie, C.E., J.P. Greenberg, and J.H. Weare. 1987. "A Chemical Equilibrium Algorithm for Highly Non-Ideal Multiphase Systems: Free Energy Minimization," *Geochimica et Cosmochimica*

Acta 51 (5) 1045-1057.

Martell, A.E., and R.M. Smith. 1977. *Critical Stability Constants, Vol.3: Other Organic Ligands*, Plenum Press, New York, New York.

Morel, F.M.M., and J.G. Hering. 1993. *Principles and Applications of Aquatic Chemistry*, John Wiley & Sons, New York, New York.

Neck, V., Th. Fanghänel, G. Rudolph, and J.I. Kim. 1995. "Thermodynamics of Neptunium(V) in Concentrated Salt Solutions: Chloride Complexation and Ion Interaction (Pitzer) Parameters for NpO^{2+} Ion," *Radiochimica Acta* 69 (1) 39-47.

Novak, C.F., and K.E. Roberts. 1995. "Thermodynamic Modeling of Neptunium(V) Solubility in Concentrated Na-CO₃-HCO₃-Cl-ClO₄-H-OH-H₂O Systems," *Scientific Basis for Nuclear Waste Management XVIII, Materials Research Society Symposium Proceedings, Kyoto, Japan, October 23-27, 1994*. Eds. T. Murakami and R.C. Ewing. Materials Research Society, Pennsylvania, PA, 353 (2) 1119-1128.

Novak, C.F., and R.C. Moore. 1996. "Estimates of Dissolved Concentrations for +III, +IV, +V and +VI Actinides in Salado and Castile Brine," Sandia National Laboratories, Albuquerque, NM. Sandia WIPP Central Files WPO# 35835.

Novak, C.F., M. Borkowski, and G.R. Choppin. 1996. "Thermodynamic Modeling of Neptunium(V)-Acetate Complexation in Concentrated NaCl Media," *Radiochimica Acta* 74 111-116.

Novak, C.F., I.A. Mahamid, K.A. Becraft, S.A. Carpenter, N. Hakem, and T. Prussin. 1997. *Measurement and Thermodynamic Modeling of Np(V) Solubility in Dilute Through Concentrated K₂CO₃ Media*. SAND96-1604J. Sandia National Laboratories, Albuquerque, NM. Sandia WIPP Central Files WPO# 44289.

Papenguth, H.W. 1996a. "Parameter Record Package for Mobile-Colloidal-Actinide Source Term. 1. Mineral Fragment Colloids." Sandia National Laboratories, Albuquerque, NM. Sandia WIPP Central Files WPO# 35850.

Papenguth, H.W. 1996b. "Parameter Record Package for Mobile-Colloidal-Actinide Source Term. 2. Actinide Intrinsic Colloids." Sandia National Laboratories, Albuquerque, NM. Sandia WIPP Central Files WPO# 35852.

Papenguth, H.W. 1996c. "Parameter Record Package for Mobile-Colloidal-Actinide Source Term. 3. Humic Substances." Sandia National Laboratories, Albuquerque, NM. Sandia WIPP Central Files WPO# 35855.

Papenguth, H.W. 1996d. "Parameter Record Package for Mobile-Colloidal-Actinide Source Term. 4. Microbes." Sandia National Laboratories, Albuquerque, NM. Sandia WIPP Central

Files WPO# 35856.

Pitzer, K.S. 1973. "Thermodynamics of Electrolytes. I. Theoretical Basis and General Equations," *Journal of Physical Chemistry* **77** (2) 268-277.

Pitzer, K.S., ed. 1991. *Activity Coefficients in Electrolyte Solutions*. 2nd Ed. CRC Press, Boca Raton, FL.

Pokrovsky, O.S., M.G. Bronikowski, R.C. Moore, and G.R. Choppin. 1998. "Interaction of Neptunyl(V) and Uranyl(VI) with EDTA in NaCl Media: Experimental Study and Pitzer Modeling," *Radiochimica Acta* **80** (1) 23-29.

Rai, D., A.R. Felmy, and R.W. Fulton. 1992a. "Solubility and Ion Activity Product of $\text{AmPO}_4 \cdot x\text{H}_2\text{O}(\text{am})$," *Radiochimica Acta* **56** (1) 7-14.

Rai, D., A.R. Felmy, R.W. Fulton, and J.L. Ryan. 1992b. "Aqueous Chemistry of Nd in Borosilicate-Glass/Water Systems," *Radiochimica Acta* **58-59** (1) 9-16.

Rai, D., A.R. Felmy, and R.W. Fulton. 1995a. "The Nd^{3+} and Am^{3+} Ion Interactions with Sulfate Ion and Their Influence on $\text{NdPO}_4(\text{c})$ Solubility," *Journal of Solution Chemistry* **24** (9) 879-895.

Rai, D., A.R. Felmy, D.A. Moore, and M.J. Mason. 1995b. "The Solubility of Th(IV) and U(IV) Hydrous Oxides in Concentrated NaHCO_3 and Na_2CO_3 Solutions," *Scientific Basis for Nuclear Waste Management XVIII, Materials Research Society Symposium Proceedings, Kyoto, Japan, October 23-27, 1994*. Eds. T. Murakami and R.C. Ewing. Materials Research Society, Pennsylvania, PA, **353** (2) 1143-1150.

Rai, D., A.R. Felmy, S.M. Sterner, D.A. Moore, M.J. Mason, and C.F. Novak. 1997. "The Solubility of Th(IV) and U(IV) Hydrous Oxides in Concentrated NaCl and MgCl_2 Solutions," *Radiochimica Acta* **79** (4) 239-247.

Ramsey, J.L., M.G. Wallace, and H.N. Jow. 1996. *Analysis Package for the Culebra Flow and Transport Calculations (Task 3) of the Performance Assessment Calculations Supporting the Compliance Certification Application (CCA), AP-019*. Analysis Package 19. Sandia National Laboratories, Albuquerque, NM. Sandia WIPP Central Files WPO# 40516.

Rao, L., D. Rai, A.R. Felmy, R.W. Fulton, and C.F. Novak. 1996. "Solubility of $\text{NaNd}(\text{CO}_3)_2 \cdot 6\text{H}_2\text{O}(\text{c})$ in Concentrated Na_2CO_3 and NaHCO_3 Solutions." *Radiochimica Acta* **75**: 141-147.

Roy, R.N., K.M. Vogel, C.E. Good, W.B. Davis, L.N. Roy, D.A. Johnson, A.R. Felmy, and K.S. Pitzer. 1992. "Activity Coefficients in Electrolyte Mixtures: $\text{HCl} + \text{ThCl}_4 + \text{H}_2\text{O}$ for 5-55°C," *Journal of Physical Chemistry* **96** (26) 11065-11072.

Sanchez, L.C., J. Liscum-Powell, J.S. Rath, and H.R. Trelue. 1997. *WIPP PA Analysis Report*

for EPAUNI: *Estimating Probability Distribution of EPA Unit Loading in the WIPP Repository for Performance Assessment Calculations, Version 1.01*. Sandia National Laboratories, Albuquerque, NM. Sandia WIPP Central Files WPO# 43843.

Siegel, M.D. 1996. "Solubility Parameters for Actinide Source Term Look-Up Tables." Sandia National Laboratories, Albuquerque, NM. Sandia WIPP Central Files WPO# 35835.

Smith, L.N., J.D. Johnson, and J.C. Helton. 1996. *Analysis Package for the Complementary Cumulative Distributive Function (CCDF) Construction (Task 7) of the Performance Assessment Calculations Supporting the Compliance Certification Application (CCA), AP-AAD*. Analysis Package AAD. Sandia National Laboratories, Albuquerque, NM. Sandia WIPP Central Files WPO# 40524.

Spencer, R.J., H.P. Eugster, and B.F. Jones. 1985. "Geochemistry of Great Salt Lake, Utah II: Pleistocene-Holocene Evolution," *Geochimica et Cosmochimica Acta* 49 (3) 739-747.

Stockman, C., A. Shinta, and J.W. Garner. 1996. *Analysis Package for the Salado Transport Calculations (Task 2) of the Performance Assessment Analyses Supporting the Compliance Certification Application (CCA), AP-023*. Analysis Package 23. Sandia National Laboratories, Albuquerque, NM. Sandia WIPP Central Files WPO# 40515.

Stoelzel, D.M., and D.G. O'Brien. 1996. *Analysis Package for the BRAGFLO Direct Release Calculations (Task 4) of the Performance Assessment Calculations Supporting the Compliance Certification Application (CCA), AP-029, Brine Release Calculations*. Analysis Package 29. Sandia National Laboratories, Albuquerque, NM. Sandia WIPP Central Files WPO# 40520.

Stumm, W. 1992. *Chemistry of the Solid-Water Interface: Processes at the Mineral-Water and Particle-Water Interface in Natural Systems*. John Wiley & Sons, New York, New York.

Vaughn, P.M. 1996. *Analysis Package for the Salado Flow Calculations (Task 1) of the Performance Assessment Analysis Supporting the Compliance Certification Application (CCA)*. Sandia National Laboratories, Albuquerque, NM. Sandia WIPP Central Files WPO# 40514.

Vold, R.D., and M.J. Vold. 1983. *Colloid and Interface Chemistry*. Addison-Wesley, Reading, MA.

Wang, Y. 1996. "Define Chemical Conditions for FMT Actinide Solubility Calculations." Sandia National Laboratories, Albuquerque, NM. Sandia WIPP Central Files WPO# 37038.

Weiner, R. 1996. "Documentation Package for Oxidation State Distribution of Actinides in the Repository." Sandia National Laboratories, Albuquerque, NM. Sandia WIPP Central Files WPO# 35194.